Single- and double-hump femtosecond vector solitons in the coupled Sasa-Satsuma system

Tao Xu* and Xiang-Min Xu
College of Science, China University of Petroleum, Beijing 102249, China
(Received 19 September 2012; revised manuscript received 10 January 2013; published 25 March 2013)

We construct the Darboux transformation of the coupled Sasa-Satsuma system and represent the N-soliton solutions in terms of the five-component Wronskian. We give the parametric criterion for the appearance of single- and double-hump soliton profiles, and analyze the structure and stability of double-hump solitons. We also reveal the polarization-changing collisions occurring in the femtosecond vector solitons with the third-order dispersion, self-steepening, and stimulated Raman scattering effects. Such nontrivial collisions may have applications in the ultrafast all-optical switching, computation, and signal control.

DOI: 10.1103/PhysRevE.87.032913 PACS number(s): 05.45.Yv, 42.65.Tg, 42.81.Dp

I. INTRODUCTION

It is known that the single-mode optical fibers are not really "single-mode" but are actually bimodal because of the birefringence induced by various imperfections randomly distributed along the fiber [1]. With the presence of the birefringence, the real fibers can support the vector solitons in which two orthogonally polarized components trap each other [2]. In the picosecond regime, the governing model for the vector solitons propagation in the birefringent or two-mode fibers is the coupled nonlinear Schrödinger (CNLS) system [2,3]. With the internal degrees of freedom, the picosecond vector solitons have been found to admit the polarization-changing collisions along with energy exchange between two components under certain parametric condition [4–8]. Such nontrivial collisions have been experimentally observed in the linearly birefringent fibers [9] and brought about some applications such as the implementation of the all-optical digital computation [10] and design of the "solitonets," which are complex networks made up of interacting fields [11].

To improve the capacity of high-bit-rate transmission systems, the propagation of femtosecond pulses with the width less than 100 fs is tempting and desirable [12]. In this case, the effects of third-order dispersion (TOD), self-steepening (SS, also known as Kerr dispersion), and stimulated Raman scattering (SRS) should be taken into account [13]. As the available laser power continues to grow, there is an increasing interest in the femtosecond soliton pulse propagation inside the birefringent fibers [14] or multimode fibers [15], and the pulse trapping generated by the femtosecond soliton pulses in the birefringent fibers [16] or across the zero-dispersion wavelength [17].

With all the effects of TOD, SS, and SRS, the dynamics of femtosecond vector solitons in the birefringent or two-mode fibers can be approximately described by the following coupled higher-order nonlinear Schrödinger (CHONLS) system [16–21]:

$$\mathrm{i}\,u_{j,z}+\frac{1}{2}u_{j,tt}+\sum_{k=1}^{2}|u_k|^2u_j+\mathrm{i}\,\varepsilon\left[u_{j,ttt}+6\sum_{k=1}^{2}|u_k|^2u_{j,t}+3\left(\sum_{k=1}^{2}|u_k|^2\right)_t u_j\right]=0,\quad (j=1,2),\tag{1}$$

which is usually referred to as the coupled Sasa-Satsuma system [22], where z and t, respectively, represent the propagation direction and retarded time, u_j corresponds to the jth optical field, ε is the ratio of the width of the spectra to the carrier frequency, and the last three terms in the left-hand side of (1) stand for the TOD, SS, and SRS effects, respectively.

System (1) is a completely integrable model in the sense of being solvable by the inverse scattering transform [23] and possesses some integrable properties such as the Bäcklund transformation [20], Painlevé property [21], and bilinear representation [24]. However, the Darboux transformation (DT) as an important aspect for indicating the integrability of system (1) has not been obtained in the previous literature. The DT applies only to the Lax-integrable nonlinear equations, but to the best of our understanding it admits the following two virtues: (1) The DT, which comprises the eigenfunction and potential transformations, can be used to recursively generate an infinite chain of solutions including the multisoliton solutions [25,26]. The DT algorithm is also very computerizable since one only need solve the associated Lax pair with a given initial potential and perform tedious but not complicated iterative operations [26]. In comparison, the Bäcklund transformation is not very straightforward in use because it just stays on the potential level but does not involve the eigenfunction transformation [25]. (2) Instead of the guesswork when using the Hirota method [27], the iterated DT algorithm enables us to easily represent the generated solutions in terms of some determinants like the Wronskian and Grammian [7,25]. Moreover, the determinant representation provides an algebraic basis for the direct verification of the solutions [7] and makes it feasible to algebraically study the collision dynamics among an arbitrary number of solitons [8,28].

In this paper, we will employ the DT method to study the femtosecond vector solitons in system (1) from the following three considerations: (a) It has been shown in Refs. [7,8] that the multicomponent Wronskian solutions can lead to an algebraic procedure to directly study the collision dynamics for an arbitrary number of vector solitons in the incoherently CNLS system. Also, it is desirable to obtain the uniform determinant representation of the general N-soliton solutions for system (1). (b) The one-component Sasa-Satsuma equation possesses the double-hump solitons [22,29] in addition to the usual single-hump solitons. It is of importance to study

*xutao@cup.edu.cn

the structure and stability of double-hump solitons in system (1) since such kind of solitons may allow higher bit-rate transmission systems based on the multilevel information-coding scheme in each pulse [30]. (c) To our knowledge, the previous studies have reported only the polarization-preserving collisions of vector solitons in system (1), as seen, e.g., in Ref. [24]. It is still an unsolved question as to whether system (1) can exhibit the polarization-changing vector-soliton collisions along with energy exchange between two components, like the case in the incoherently CNLS system [4–8].

II. DARBOUX TRANSFORMATION AND *N*-SOLITON SOLUTIONS

To begin with, we introduce the variable transformations [22]

$$u_j(t,z) = q_j(T,Z)\mathrm{e}^{\mathrm{i}\left(\frac{t}{6\varepsilon}-\frac{z}{108\varepsilon^2}\right)} \quad (j=1,2), \quad Z=\varepsilon z, \quad T = t-\frac{z}{12\varepsilon} \tag{2}$$

to convert system (1) into the following coupled complex modified Korteweg-de Vries system:

$$q_{j,Z}+q_{j,TTT}+6\sum_{k=1}^{2}|q_k|^2q_{j,T}+3\left(\sum_{k=1}^{2}|q_k|^2\right)_T q_j=0 \quad (j=1,2). \tag{3}$$

The Lax pair of system (3) can be written in the 5×5 Ablowitz-Kaup-Newell-Segur form [20]:

$$\Psi_T=\begin{pmatrix}\lambda & \mathbf{Q}\\ -\mathbf{Q}^\dagger & -\lambda E_4\end{pmatrix}\Psi, \quad \mathbf{Q}=(q_1,q_2,q_3,q_4), \tag{4a}$$

$$\Psi_Z=\begin{pmatrix}-4\lambda^3-2\lambda\mathbf{Q}\mathbf{Q}^\dagger+\mathbf{Q}\mathbf{Q}_T^\dagger-\mathbf{Q}_T\mathbf{Q}^\dagger & -4\lambda^2\mathbf{Q}-2\lambda\mathbf{Q}_T-\mathbf{Q}_{TT}-2\mathbf{Q}\mathbf{Q}^\dagger\mathbf{Q}\\ 4\lambda^2\mathbf{Q}^\dagger-2\lambda\mathbf{Q}_T^\dagger+\mathbf{Q}_{TT}^\dagger+2\mathbf{Q}^\dagger\mathbf{Q}\mathbf{Q}^\dagger & 4\lambda^3E_4-2\lambda\mathbf{Q}^\dagger\mathbf{Q}+\mathbf{Q}^\dagger\mathbf{Q}_T-\mathbf{Q}_T^\dagger\mathbf{Q}\end{pmatrix}\Psi, \tag{4b}$$

with the complementary constraints

$$q_3=q_1^*, \quad q_4=q_2^*, \tag{5}$$

where $\Psi=(\psi_1,\psi_2,\psi_3,\psi_4,\psi_5)^{\mathrm{T}}$ (T represents the transpose of a vector) is the vector eigenfunction, λ is the spectral parameter, E_4 is the 4×4 identity matrix, and the asterisk and dagger, respectively, denote the complex conjugate and Hermitian conjugate (i.e., transpose and conjugate).

Without consideration of constraints (5), the compatibility condition $\Psi_{TZ}=\Psi_{ZT}$ yields

$$q_{j,Z}+q_{j,TTT}+3\sum_{k=1}^{4}|q_k|^2q_{j,T}+3\sum_{k=1}^{4}q_{k,T}q_k^*q_j=0, \quad (1\leqslant j\leqslant 4), \tag{6}$$

which is equivalent to the four-coupled Hirota system, which is also an integrable CHONLS system excluding the SRS term [31]. In the manner of Ref. [32], the Mth iterated DT for system (6) can be constituted by the eigenfunction transformation

$$\Psi_M=[\lambda^M E_5-S_M(\lambda)]\Psi, \tag{7a}$$

$$S_M(\lambda)=\begin{pmatrix}\sum_{n=0}^{M-1}a_n\lambda^n & -\sum_{n=0}^{M-1}b_{1n}(-\lambda)^n & \cdots & -\sum_{n=0}^{M-1}b_{4n}(-\lambda)^n\\ \sum_{n=0}^{M-1}c_{1n}\lambda^n & -\sum_{n=0}^{M-1}d_{11}^{(n)}(-\lambda)^n & \cdots & -\sum_{n=0}^{M-1}d_{14}^{(n)}(-\lambda)^n\\ \vdots & \vdots & \ddots & \vdots\\ \sum_{n=0}^{M-1}c_{4n}\lambda^n & -\sum_{n=0}^{M-1}d_{41}^{(n)}(-\lambda)^n & \cdots & -\sum_{n=0}^{M-1}d_{44}^{(n)}(-\lambda)^n\end{pmatrix}, \tag{7b}$$

and the potential transformation

$$q_{j,M}=q_j+2(-1)^M b_{j,M-1}, \tag{8}$$

where the subscript M is a mark to signify the Mth iterated DT. The functions $a_n(T,Z)$, $b_{jn}(T,Z)$, $c_{in}(T,Z)$, and $d_{ij}^{(n)}(T,Z)$ $(1\leqslant i,j\leqslant 4;\ 0\leqslant n\leqslant M-1)$ satisfy the conditions

$$S_M(\lambda_k)\Phi_k=\lambda_k^M\Phi_k, \quad S_M(-\lambda_k^*)\Omega_k^{(j)}=(-\lambda_k^*)^M\Omega_k^{(j)} \quad (1\leqslant j\leqslant 4;\ 1\leqslant k\leqslant M), \tag{9}$$

where $\Phi_k=(f_k,g_k^{(1)},g_k^{(2)},g_k^{(3)},g_k^{(4)})^{\mathrm{T}}$ is the solution of Lax pair (4a) and (4b) with $\lambda=\lambda_k$ ($\lambda_k\neq\lambda_l$ for $k\neq l$), $\Omega_k^{(j)}=(-g_k^{(j)*},\overbrace{0,\ldots,0}^{j-1},f_k^*,\overbrace{0,\ldots,0}^{4-j})^{\mathrm{T}}$ $(1\leqslant j\leqslant 4)$ are the vector functions orthogonal to Φ_k.

Since $\{\Phi_k\}_{k=1}^M$ and $\{\Omega_k^{(j)}\}_{k=1}^M$ $(1\leqslant j\leqslant 4)$ are five sets of linearly independent solutions, the elements in $S_M(\lambda)$ can be uniquely determined from Eq. (9) by Cramer's rule. In order to maintain the complex conjugate constraints $q_{3M}=q_{1M}^*$ and $q_{4M}=q_{2M}^*$, we still require that

$$M=2N, \quad \lambda_{N+k}=\lambda_k^*, \tag{10a}$$

$$\Phi_{N+k}=\left(f_k^*,g_k^{(3)*},g_k^{(4)*},g_k^{(1)*},g_k^{(2)*}\right)^{\mathrm{T}},$$

$$\Omega_{N+k}^{(j)}=\left(-g_k^{(j')},\overbrace{0,\ldots,0}^{j-1},f_k,\overbrace{0,\ldots,0}^{4-j}\right)^{\mathrm{T}}, \tag{10b}$$

where $1 \leqslant k \leqslant N$, $j' = j + 2$ (modulo 4), $\Omega_{N+k}^{(j)}$ $(1 \leqslant j \leqslant 4)$ are all orthogonal to Φ_{N+k}. With the reduction in Eqs. (10a) and (10b), transformations (7) and (8) are reduced to the Nth iterated DT for system (3) [or equivalently system (1)], which has been presented here for the first time.

We implement the above DT algorithm starting from $q_j = 0$ $(j = 1,2)$. With $\lambda = \lambda_k$ $(1 \leqslant k \leqslant N)$, the solutions of Lax pair (4a) and (4b) can be given as

$$\left(f_k, g_k^{(1)}, g_k^{(2)}, g_k^{(3)}, g_k^{(4)}\right) = (\alpha_k e^{\theta_k}, \beta_k e^{-\theta_k}, \gamma_k e^{-\theta_k}, \delta_k e^{-\theta_k}, \sigma_k e^{-\theta_k}), \tag{11}$$

with $\theta_k = \lambda_k(t - \frac{z}{12\varepsilon}) - 4\varepsilon\lambda_k^3 z$, and α_k, β_k, γ_k, δ_k, and σ_k $(1 \leqslant k \leqslant N)$ are all complex constants. Particularly taking $\delta_k = \sigma_k = 0$ for $1 \leqslant k \leqslant N$, we use transformation (8) to obtain the N-soliton solutions of system (1) in terms of the following five-component Wronskian:

$$\begin{aligned} u_1 &= -2\, e^{i\left(\frac{t}{6\varepsilon} - \frac{z}{108\varepsilon^2}\right)} \frac{\tau_{2N+1,2N-1,2N}}{\tau_{2N,2N,2N}}, \\ u_2 &= -2\, e^{i\left(\frac{t}{6\varepsilon} - \frac{z}{108\varepsilon^2}\right)} \frac{\tau_{2N+1,2N,2N-1}}{\tau_{2N,2N,2N}} \end{aligned} \tag{12}$$

with

$$\tau_{J,K,L} = \begin{vmatrix} F_{N\times J} & -G_{N\times K} & -H_{N\times L} & \mathbf{0} & \mathbf{0} \\ F^*_{N\times J} & \mathbf{0} & \mathbf{0} & -G^*_{N\times 2N} & -H^*_{N\times 2N} \\ G^*_{N\times J} & F^*_{N\times K} & \mathbf{0} & \mathbf{0} & \mathbf{0} \\ \mathbf{0} & F_{N\times K} & \mathbf{0} & \mathbf{0} & \mathbf{0} \\ H^*_{N\times J} & \mathbf{0} & F^*_{N\times L} & \mathbf{0} & \mathbf{0} \\ \mathbf{0} & \mathbf{0} & F_{N\times L} & \mathbf{0} & \mathbf{0} \\ \mathbf{0} & \mathbf{0} & \mathbf{0} & F^*_{N\times 2N} & \mathbf{0} \\ G_{N\times J} & \mathbf{0} & \mathbf{0} & F_{N\times 2N} & \mathbf{0} \\ \mathbf{0} & \mathbf{0} & \mathbf{0} & \mathbf{0} & F^*_{N\times 2N} \\ H_{N\times J} & \mathbf{0} & \mathbf{0} & \mathbf{0} & F_{N\times 2N} \end{vmatrix} \tag{13}$$

where $J + K + L = 6N$, the matrices $F_{N\times J}$, $G_{N\times K}$, and $H_{N\times L}$ are given by

$$\begin{aligned} F_{N\times J} &= A\Theta_+\Lambda_{+,J}, \quad G_{N\times K} = B\Theta_-\Lambda_{-,K}, \\ H_{N\times L} &= C\Theta_-\Lambda_{-,L}, \end{aligned} \tag{14}$$

$A = \mathrm{diag}(\alpha_1, \ldots, \alpha_N)$, $B = \mathrm{diag}(\beta_1, \ldots, \beta_N)$, $C = \mathrm{diag}(\gamma_1, \ldots, \gamma_N)$, $\Theta_+ = \mathrm{diag}(e^{\theta_1}, \ldots, e^{\theta_N})$, $\Theta_- = \mathrm{diag}(e^{-\theta_1}, \ldots, e^{-\theta_N})$, $\Lambda_{+,J} = (\lambda_n^{m-1})_{N\times J}$, $\Lambda_{-,K} = [(-\lambda_n)^{m-1}]_{N\times K}$, $\Lambda_{-,L} = [(-\lambda_n)^{m-1}]_{N\times L}$. Without loss of generality, we can take $\alpha_k = 1$ for $1 \leqslant k \leqslant N$ [32]. It means that the N-soliton solutions of system (1) are in general characterized by $3N$ complex parameters $\{\beta_k, \gamma_k, \lambda_k\}_{k=1}^N$, which is the same as the case for the incoherently CNLS system [4–8].

III. NONDEGENERATE VECTOR SOLITONS AND POLARIZATION-CHANGING COLLISIONS

For $\lambda_{1I} = 0$, solutions (12) with $N = 1$ represent only the single-hump solitons of the "sech" profile, which have been discussed in Refs. [20,24]. If $\lambda_{1I} \neq 0$, solutions (12) with $N = 1$ can be written as

$$\begin{aligned} \begin{pmatrix} u_1 \\ u_2 \end{pmatrix} = \begin{pmatrix} \beta_1^* \\ \gamma_1^* \end{pmatrix} & \frac{2e^{i\left(\frac{t}{6\varepsilon} - \frac{z}{108\varepsilon^2}\right)} \lambda_{1R} e^{\theta_1 - \theta_1^*}}{2|\lambda_{1I}| \cosh^2\left(\xi_1 + \ln\sqrt{\frac{|\lambda_{1I}|}{|\lambda_1|\Delta_1}}\right) + |\lambda_1| - |\lambda_{1I}|} \\ & \times \left\{ [|\lambda_1| - i\lambda_1^* \mathrm{sgn}(\lambda_{1I})] e^{-\xi_1} + 2i\lambda_1^* \mathrm{sgn}(\lambda_{1I}) \right. \\ & \left. \times \sqrt{\frac{|\lambda_{1I}|}{|\lambda_1|\Delta_1}} \cosh\left(\xi_1 + \ln\sqrt{\frac{|\lambda_{1I}|}{|\lambda_1|\Delta_1}}\right) \right\}, \end{aligned} \tag{15}$$

with $\xi_1 := \theta_1 + \theta_1^*$, $\Delta_1 := |\beta_1|^2 + |\gamma_1|^2$, where λ_{1R} and λ_{1I} denote the real and imaginary parts of λ_1, respectively. Because $\lambda_{1I} \neq 0$, one more degree of freedom is added in solutions (15). Thus, solutions (15) are nondegenerate in the sense that they can display both the single- and double-hump soliton profiles under different parametric conditions. In the manner of Ref. [22], we take the derivatives of $|u_j|^2$ $(j = 1,2)$ with respect to ξ_1, yielding

$$\begin{aligned} \frac{d}{d\xi_1}\begin{pmatrix} |u_1|^2 \\ |u_2|^2 \end{pmatrix} = \begin{pmatrix} |\beta_1|^2 \\ |\gamma_1|^2 \end{pmatrix} & \frac{-32|\lambda_1|^2\lambda_{1R}^2 e^{2\xi_1}\left(\lambda_{1I}^2 e^{4\xi_1} - |\lambda_1|^2\Delta_1^2\right)}{\left(\lambda_{1I}^2 e^{4\xi_1} + 2|\lambda_1|^2\Delta_1 e^{2\xi_1} + |\lambda_1|^2\Delta_1^2\right)^3} \\ & \times \left[\lambda_{1I}^2 e^{4\xi_1} + 2\Delta_1\left(\lambda_{1I}^2 - \lambda_{1R}^2\right)e^{2\xi_1} + |\lambda_1|^2\Delta_1^2\right], \end{aligned} \tag{16}$$

which suggests that the number of extrema of $|u_j|^2$ $(j = 1,2)$ in solutions (15) is only related to λ_1; that is, the appearance of single- or double-hump soliton structure is completely dependent on the parameter λ_1.

If $|\lambda_{1R}| \leqslant \sqrt{3}|\lambda_{1I}|$, $|u_j|^2$ has only one maximum which is along the line $\mathcal{C}_0 : \theta_1 + \theta_1^* = \frac{1}{2}\ln\frac{|\lambda_1|\Delta_1}{|\lambda_{1I}|}$. Figure 1 presents three types of single-hump solitons with λ_1 satisfying $|\lambda_{1R}| \leqslant \sqrt{3}|\lambda_{1I}|$. It can be observed that the top of $|u_j|^2$ becomes flatter as $|\lambda_{1R}|$ approaches to $\sqrt{3}|\lambda_{1I}|$. For the case $|\lambda_{1R}| > \sqrt{3}|\lambda_{1I}|$, the nondegenerate soliton solutions (15) exhibit two humps whose centers are located along two lines in the tz plane:

$$\mathcal{C}_{1,2} : \theta_1 + \theta_1^* = \frac{1}{2}\ln\frac{\Delta_1\left(\lambda_{1R}^2 - \lambda_{1I}^2\right) \pm \Delta_1|\lambda_{1R}|\sqrt{\lambda_{1R}^2 - 3\lambda_{1I}^2}}{\lambda_{1I}^2}. \tag{17}$$

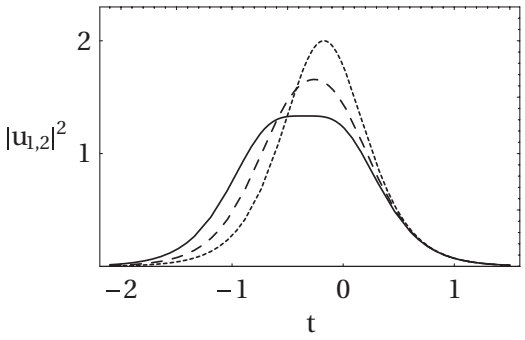

FIG. 1. Nondegenerate single-hump solitons via solutions (15) transverse at $Z = 0$, with $\varepsilon = \frac{1}{2}$, $\beta_1 = 1$, $\gamma_1 = i$, and $\lambda_1 = -1 + i\lambda_{1I}$. The dotted, dashed, and solid lines correspond to $\lambda_{1I} = -100$, $\lambda_{1I} = -1$, and $\lambda_{1I} = -\frac{1}{\sqrt{3}}$, respectively. The components u_1 and u_2 have the same intensity.

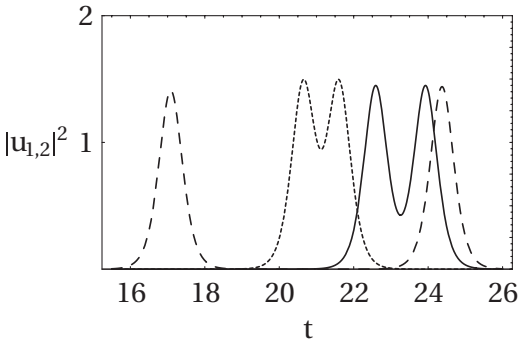

FIG. 2. Nondegenerate double-hump solitons via solutions (15) transverse at $Z = 8$, with $\varepsilon = \frac{1}{2}$, $\beta_1 = 1$, $\gamma_1 = \mathrm{i}$, and $\lambda_1 = -1.2 + \mathrm{i}\lambda_{1I}$. The dotted, dashed, and solid lines correspond to $\lambda_{1I} = -\frac{6}{25}$, $\lambda_{1I} = -\frac{24}{250}$, and $\lambda_{1I} = -6 \times 10^{-8}$, respectively. The components u_1 and u_2 have the same intensity.

At any given z, the separation between two humps is fixed and can be exactly calculated by the formula

$$d = \left| \frac{1}{4\lambda_{1R}} \ln \frac{\lambda_{1R}^2 - \lambda_{1I}^2 + |\lambda_{1R}|\sqrt{\lambda_{1R}^2 - 3\lambda_{1I}^2}}{\lambda_{1R}^2 - \lambda_{1I}^2 - |\lambda_{1R}|\sqrt{\lambda_{1R}^2 - 3\lambda_{1I}^2}} \right|, \qquad (18)$$

where $|\lambda_{1R}| > \sqrt{3}|\lambda_{1I}|$. Via the qualitative analysis, we find that the double-hump solitons obey the following three features: (i) The two humps in $|u_j|^2$ are symmetric with respect to the line $\mathcal{C}_0$ and have the same height. (ii) The soliton does not change its shape and retains the separation between two humps during the propagation. (iii) Formula (18) implies that when λ_{1R} is fixed, the separation of one hump from the other one becomes larger as λ_{1I} tends to zero (see Fig. 2).

For $N \geqslant 2$, we try to explore the polarization-changing collisions of the nondegenerate vector solitons via solutions (12) with $\lambda_{kI} \neq 0$ $(1 \leqslant k \leqslant N)$. The two-soliton solutions [i.e., solutions (12) with $N = 2$] will be studied by the multicomponent Wronskian-based asymptotic analysis technique [7,8]. As $z \to -\infty$ or $z \to \infty$, solutions (12) with $N = 2$ can be understood as a combination of two vector one-soliton solutions, whose asymptotic expressions differ from solutions (15) in the amplitudes and phases. For convenience, we define $\mathbf{a}_k = \frac{1}{\sqrt{\Delta_k}}(\beta_k, \gamma_k)^{\mathrm{T}}$ $(\Delta_k = |\beta_k|^2 + |\gamma_k|^2, k = 1,2)$ as the initial polarization vectors of two colliding solitons, and use $S_{1n}^{\pm}$ and $S_{2n}^{\pm}$ $(n = 1,2)$ to represent the nth colliding soliton in the components u_1 and u_2 as $z \to \pm\infty$, respectively.

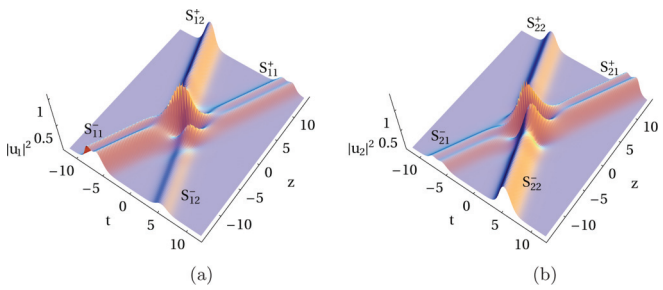

FIG. 3. (Color online) Polarization-changing collisions between single- and double-hump vector solitons via solutions (12) with $N = 2$, $\varepsilon = \frac{3}{10}$, $\beta_1 = 2$, $\beta_2 = 1$, $\gamma_1 = 1 + \mathrm{i}$, $\gamma_2 = 1 + 2\mathrm{i}$, $\lambda_1 = \frac{1}{2} + \frac{1}{6}\mathrm{i}$, and $\lambda_2 = -\frac{1}{2} - \frac{1}{2}\mathrm{i}$.

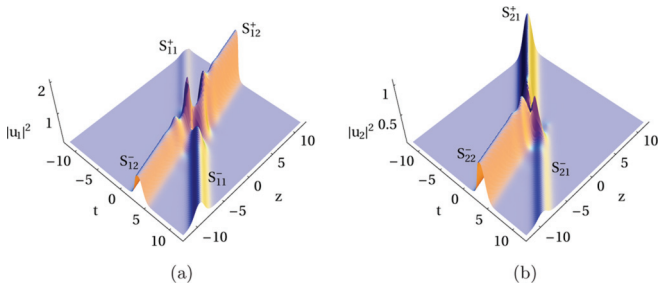

FIG. 4. (Color online) Polarization-changing collisions between two single-hump vector solitons via solutions (12) with $N = 2$, $\varepsilon = \frac{1}{2}$, $\beta_1 = \beta_2 = 1$, $\gamma_1 = \frac{1}{2}$, $\gamma_2 = 0$, $\lambda_1 = \frac{1}{2} - \frac{1}{2}\mathrm{i}$, and $\lambda_2 = \frac{3}{4} - \frac{1}{2}\mathrm{i}$. Note that the u_2 component of the second colliding soliton, i.e., S_{22}^+, completely vanishes after collision.

Our asymptotic analysis shows that the polarization-changing collisions of vector solitons can take place in system (1) if neither $\mathbf{a}_1 \parallel \mathbf{a}_2$ nor $\mathbf{a}_1 \perp \mathbf{a}_2^*$ is satisfied. In this case, the colliding vector solitons experience the polarization rotation and energy exchange between two components, but the total energy of each vector soliton in two components is conserved and exactly equals to $4|\lambda_{nR}|$ $(n = 1,2)$. Similar to the vector soliton collisions in the incoherently CNLS system [4,8], the polarization-changing collisions lead to the enhancement of intensity in one component of individual soliton, and the suppression of intensity in the other component of the corresponding soliton, as seen in Figs. 3–5. It is even possible that the intensity for one component of some vector soliton becomes zero after collision; for example, $\gamma_2 = 0$ (or $\beta_2 = 0$) causes the disappearance of S_{22}^+ (or S_{12}^+) in Fig. 4(b) [or Fig. 5(a)].

On the other hand, under the parametric condition $\mathbf{a}_1 \parallel \mathbf{a}_2$ or $\mathbf{a}_1 \perp \mathbf{a}_2^*$ both components of each vector soliton preserve their polarizations and velocities after collision except for the phase shifts. Particularly, in the case $\beta_n = \gamma_{3-n} = 0$ $(n = 1,2)$, which is in obedience to $\mathbf{a}_1 \perp \mathbf{a}_2^*$, either colliding vector soliton has one component absent after collision. Because the nonvanishing components belong to two different vector solitons, they experience a phase shift upon their mutual interaction, as shown in Fig. 6. In the context of birefringent

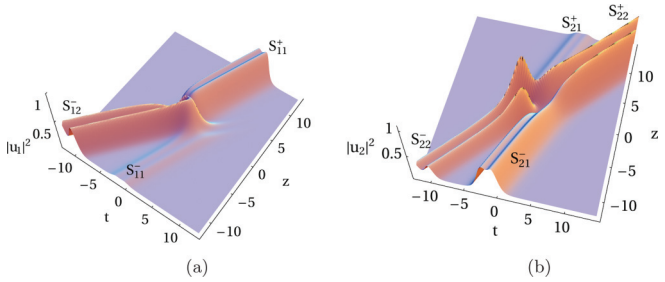

FIG. 5. (Color online) Polarization-changing collisions between two double-hump vector solitons via solutions (12) with $N = 2$, $\varepsilon = \frac{1}{2}$, $\beta_1 = \frac{1}{3}$, $\beta_2 = 0$, $\gamma_1 = 1$, $\gamma_2 = 1$, $\lambda_1 = \frac{1}{2} - \frac{1}{5}\mathrm{i}$, and $\lambda_2 = \frac{3}{5} - \frac{1}{10}\mathrm{i}$. Note that the u_1 component of the second colliding soliton, i.e., S_{12}^+, completely vanishes after collision.

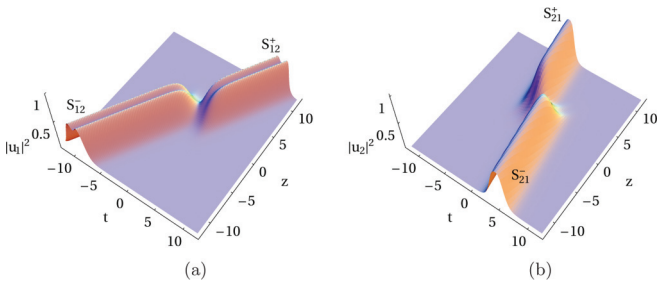

FIG. 6. (Color online) Particular polarization-preserving collisions between single- and double-hump vector solitons via solutions (12) with $N = 2$, $\varepsilon = \frac{4}{5}$, $\beta_1 = 0$, $\beta_2 = 1$, $\gamma_1 = 1$, $\gamma_2 = 0$, $\lambda_1 = -\frac{1}{2} - \frac{1}{3}$i, and $\lambda_2 = \frac{1}{2} + \frac{1}{6}$i. Note that the soliton components shown in (a) and (b) belong to two different vector solitons, respectively.

or two-mode fibers, this corresponds to the case of two optical soliton pulses with different frequencies and wave numbers propagating in their individual components.

IV. DISCUSSION

1. It is because the presence of the SRS term that system (1) admits both the single- and double-hump soliton profiles. We should also mention a common property for the single- and double-hump solitons in solutions (15); that is, the central position of the soliton depends on λ_1 in addition to β_1 and γ_1. Therefore, the variation of λ_1 may cause the position shift of the soliton, as displayed in Figs. 1 and 2. Note that the coupled Hirota system [31] does not exhibit this property due to the absence of the SRS term [32].

2. We note that in the incoherently CNLS system the two vector solitons can form a bound state with periodic attraction and repulsion if the they have the same velocity [30]. Such two-vector-soliton bound state exhibits the periodically varying double-hump structure except that the two solitons are both nonpropagating [33]. Differently, the symmetric double-hump soliton profile in solutions (15) is always retained during the propagation if the condition $|\lambda_{1R}| > \sqrt{3}|\lambda_{1I}|$ is satisfied. Accordingly, solutions (15) with $|\lambda_{1R}| > \sqrt{3}|\lambda_{1I}|$ represent only a one-vector soliton having two symmetric humps, but not a pair of solitons with a constant distance between each other. Besides, it has been found that the coherently CNLS system also admits such a kind of soliton solutions [34,35]. However, the polarization-changing collisions between double-hump solitons cannot occur in the coherently CNLS system, and its double-hump soliton may change into a single-hump one when interacting with the degenerate soliton [34,35].

3. In the context of fiber optics, the parameters λ_{1R} and λ_{1I} are respectively related to the soliton energy and frequency shift from the carrier frequency [12]. That implies that the formation of single- or double-hump soliton requires an elaborate design of the power and width of the input pulse. By the split-step Fourier method [12], we make a numerical simulation of system (1) with solutions (15) at $z = 0$ as the initial coupled pulses. Figure 7(a) shows that a double-hump soliton propagates stably over four dispersion lengths along the fiber. To study the stability of the double-hump soliton against a small perturbation from some fiber parameters, we assume that the initial pulses have a 10% deviation from the exact solutions (15) at $z = 0$. As seen in Figs. 7(b) and 7(c), such a small perturbation does not destroy the double-hump structure and affects the stability of the pulses slightly. For a more detailed analysis, one need employ the soliton perturbation theory [36] to give a definite answer on whether there exists a certain region in which the double-hump solitons are stable.

4. As seen from solutions (15), both the single- and double-hump solitons satisfy the boundary condition $u_1 = u_2 = 0$ as $|t| \to \infty$. In practice, the periodic boundary condition is acceptable if the pulse width is considerably short [12]. On the other hand, it is hard to produce the double-hump pulse soliton with the present laser technology. As suggested in Ref. [37], a feasible way is to utilize the initial antiphase coupled Gaussian pulses

$$u_1(0,t) = u_2(0,t) = f\left(t - \frac{T_s}{2}\right) - f\left(t + \frac{T_s}{2}\right), \quad (19)$$

with $f(t) = \sqrt{\frac{E_0 p_0}{\sqrt{\pi}}} e^{-\frac{p_0^2}{2} t^2}$, where E_0, T_s, and p_0 respectively stand for the pulse energy, spacing and width, "−" defines the anti-phase relation between two pulses. However, it requires to be further studied whether the coupled pulses defined in (19) can propagate stably over a fiber distance long enough.

5. In the optical communication lines, the binary data "1" and "0" can be respectively represented by the presence and absence of an optical soliton, and thus the digital communication bit depends on the proximity of neighboring solitons [12]. The double-hump solitons may be appropriate candidates for the multilevel communication in the birefringent or two-mode

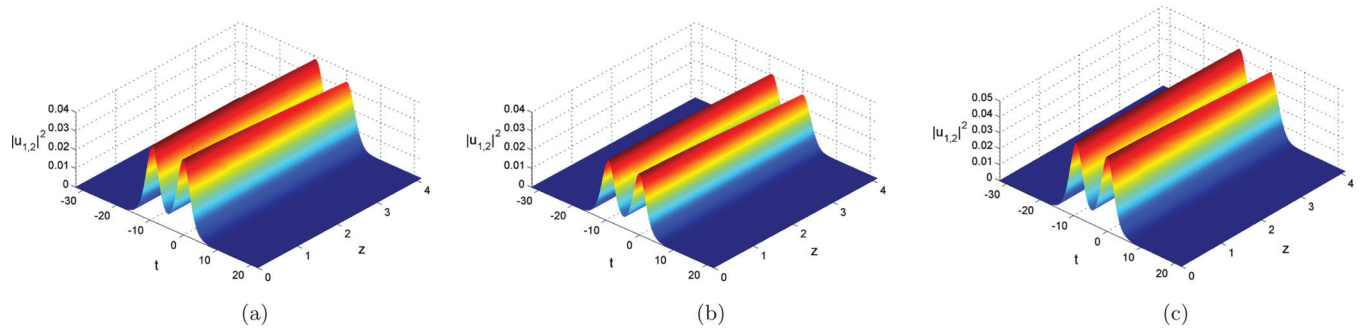

FIG. 7. (Color online) Numerical simulations for the evolution of the coupled double-hump pulses, where the components u_1 and u_2 have the same intensity. (a) The initial pulses correspond to the exact solutions (15) at $z = 0$ with $\beta_1 = \gamma_1 = 1$, $\lambda_1 = -0.2 - 0.01$i, and $\varepsilon = 0.1$. (b) The initial pulses are 10% less than the exact solutions. (c) The initial pulses are 10% greater than the exact solutions.

fibers [30]. In fact, it has been experimentally found that the double-hump solitons are immune to the time position shifts arising from intrachannel interactions in the dispersion-managed system [37]. This property leads to the invention of an error preventable line-coding scheme in which the binary data are assigned to the single- and double-hump solitons [37].

6. In view of the elegant properties of the five-component Wronskian in (13), one can continue to study the collisions among three or more vector solitons on the symbolic computation platform like Mathematica [8,32]. It is natural to infer that the polarization-changing collisions occur in the N-soliton solutions (12) if $\mathbf{a}_k$ is neither parallel to $\mathbf{a}_l$ nor orthogonal to $\mathbf{a}_l^*$ ($k \neq l$). The polarization-changing collisions of femtosecond vector solitons in system (1) may have potential applications in the ultrafast all-optical virtual logic and computation [10], high-performance all-optical switching [18], highly-functional all-optical signal regenerator [19], and higher bit-rate optical fiber complex network [11,38].

V. CONCLUSIONS

In this paper we have constructed the iterated DT for system (1) and revealed that its N-soliton solutions can be uniformly represented in terms of the five-component Wronskian in (13). Such determinant representation makes it possible to study the properties and collision behaviors of femtosecond vector solitons in an algebraic way. We have given the parametric criterion for the appearance of single- and double-hump soliton profiles in system (1) and analyzed the structure and stability of double-hump solitons. Moreover, we have found that the vector solitons in system (1) can exhibit the polarization-changing collisions and obtained the parametric condition for the occurrence of such nontrivial collisions. It is expected that the double-hump solitons and their polarization-changing collisions can be experimentally observed in the birefringent or two-mode optical fibers with the TOD, SS, and SRS effects.

ACKNOWLEDGMENTS

This work has been supported by the Science Foundations of China University of Petroleum, Beijing (Grants No. BJ-2011-04 and JCXK-2011-09), and by the Special Funds of the National Natural Science Foundation of China (Grant No. 11247267).

[1] I. P. Kaminow, IEEE J. Quantum Electron. **17**, 15 (1981).
[2] C. R. Menyuk, Opt. Lett. **12**, 614 (1987).
[3] S. V. Manakov, Sov. Phys. JETP **38**, 248 (1974).
[4] R. Radhakrishnan, M. Lakshmanan, and J. Hietarinta, Phys. Rev. E **56**, 2213 (1997).
[5] M. J. Ablowitz, B. Prinari, and A. D. Trubatch, Inverse Probl. **20**, 1217 (2004).
[6] M. Soljačić, K. Steiglitz, S. M. Sears, M. Segev, M. H. Jakubowski, and R. Squier, Phys. Rev. Lett. **90**, 254102 (2003).
[7] T. Xu and B. Tian, J. Phys. A **43**, 245205 (2010); J. Math. Phys. **51**, 033504 (2010).
[8] T. Xu, B. Tian, Y. S. Xue, and F. H. Qi, Europhys. Lett. **92**, 50002 (2010).
[9] D. Rand, I. Glesk, C. S. Brès, D. A. Nolan, X. Chen, J. Koh, J. W. Fleischer, K. Steiglitz, and P. R. Prucnal, Phys. Rev. Lett. **98**, 053902 (2007).
[10] M. H. Jakubowski, K. Steiglitz, and R. Squier, Phys. Rev. E **58**, 6752 (1998).
[11] I. Kaminer, M. Segev, A. M. Bruckstein, and Y. C. Eldar, Proc. R. Soc. A **465**, 1093 (2009).
[12] G. P. Agrawal, *Nonlinear Fiber Optics*, 3rd ed. (Academic Press, San Diego, 2002).
[13] Y. Kodama, J. Stat. Phys. **39**, 597 (1985).
[14] Y. J. Chen and J. Atai, J. Opt. Soc. Am. B **14**, 2365 (1997).
[15] F. Poletti and P. Horak, J. Opt. Soc. Am. B **25**, 1645 (2008).
[16] N. Nishizawa and T. Goto, Opt. Express **10**, 256 (2002).
[17] N. Nishizawa and T. Goto, Opt. Lett. **27**, 152 (2002).
[18] N. Nishizawa and T. Goto, Opt. Express **11**, 359 (2003).
[19] E. Shiraki, N. Nishizawa, and K. Itoh, J. Opt. Soc. Am. B **28**, 2643 (2011).
[20] K. Nakkeeran, K. Porsezian, P. S. Sundaram, and A. Mahalingam, Phys. Rev. Lett. **80**, 1425 (1998).
[21] K. Porsezian, P. Shanmugha Sundaram, and A. Mahalingam, Phys. Rev. E **50**, 1543 (1994).
[22] N. Sasa and J. Satsuma, J. Phys. Soc. Jpn. **60**, 409 (1991).
[23] S. Nandy, Nucl. Phys. B **679**, 647 (2004).
[24] M. N. Vinoj and V. C. Kuriakose, Phys. Rev. E **62**, 8719 (2000).
[25] V. B. Matveev and M. A. Salle, *Darboux Transformations and Solitons* (Springer, Berlin, 1991).
[26] C. H. Gu, H. S. Hu, and Z. X. Zhou, *Darboux Transformation in Soliton Theory and Its Geometric Applications* (Shanghai Scientific and Technical Publishers, Shanghai, 2005).
[27] R. Hirota, *The Direct Method in Soliton Theory* (Cambridge University Press, Cambridge, 2004).
[28] G. Biondini and S. Chakravarty, J. Math. Phys. **47**, 033514 (2006).
[29] J. Yang, *Nonlinear Waves in Integrable and Nonintegrable Systems* (SIAM, Philadelphia, 2010).
[30] N. Akhmediev and A. Ankiewicz, Chaos **10**, 600 (2000).
[31] R. S. Tasgal and M. J. Potasek, J. Math. Phys. **33**, 1208 (1992).
[32] T. Xu, B. Tian, and F. H. Qi, Z. Naturforsch. **67a**, 39 (2012).
[33] Z. Y. Sun, Y. T. Gao, X. Yu, W. J. Liu, and Y. Liu, Phys. Rev. E **80**, 066608 (2009).
[34] T. Kanna, M. Vijayajayanthi, and M. Lakshmanan, J. Phys. A **43**, 434018 (2010).
[35] T. Xu, P. P. Xin, Y. Zhang, and J. Li, Z. Naturforsch. **68a**, 261 (2013).
[36] J. Yang, Phys. Rev. E **59**, 2393 (1999).
[37] A. Maruta, T. Inoue, Y. Nonaka, and Y. Yoshika, IEEE J. Sel. Top. Quantum Electron. **8**, 640 (2002); X. S. Mao and A. Maruta, IEICE Trans. Commun. **E88-B**, 1955 (2005).
[38] C. Yeh and L. Bergman, Phys. Rev. E **57**, 2398 (1998).